ARMY RESEARCH LABORATORY

Model-guided Examination of Human Signatures Produced by an Array-based Radar System

by Kenneth Ranney, Calvin Le, Getachew Kirose, and Anders Sullivan

ARL-TN-0377 **November 2009**

NOTICES

Disclaimers

The findings in this report are not to be construed as an official Department of the Army position unless so designated by other authorized documents.

Citation of manufacturer's or trade names does not constitute an official endorsement or approval of the use thereof.

Destroy this report when it is no longer needed. Do not return it to the originator.

Army Research Laboratory
Adelphi, MD 20783-1197

ARL-TN-0377 **November 2009**

Model-guided Examination of Human Signatures Produced by an Array-based Radar System

Kenneth Ranney, Calvin Le, Getachew Kirose, and Anders Sullivan
Sensors and Electron Devices Directorate, ARL

REPORT DOCUMENTATION PAGE

Form Approved
OMB No. 0704-0188

1. REPORT DATE *(DD-MM-YYYY)*	2. REPORT TYPE	3. DATES COVERED (From - To)
November 2009		

4. TITLE AND SUBTITLE
Model-guided Examination of Human Signatures Produced by an Array-based Radar System

5a. CONTRACT NUMBER

5b. GRANT NUMBER

5c. PROGRAM ELEMENT NUMBER

6. AUTHOR(S)
Kenneth Ranney, Calvin Le, Getachew Kirose, and Anders Sullivan

5d. PROJECT NUMBER

5e. TASK NUMBER

5f. WORK UNIT NUMBER

7. PERFORMING ORGANIZATION NAME(S) AND ADDRESS(ES)
U.S. Army Research Laboratory
ATTN: RDRL-SER-U
2800 Powder Mill Road
Adelphi, MD 20783-1197

8. PERFORMING ORGANIZATION REPORT NUMBER
ARL-TN-0377

9. SPONSORING/MONITORING AGENCY NAME(S) AND ADDRESS(ES)

10. SPONSOR/MONITOR'S ACRONYM(S)

11. SPONSOR/MONITOR'S REPORT NUMBER(S)

12. DISTRIBUTION/AVAILABILITY STATEMENT
Approved for public release; distribution unlimited.

13. SUPPLEMENTARY NOTES

14. ABSTRACT
We adapt X-patch models and processing to produce moving target indication (MTI) signatures that better represent those produced by an array-based system. We then consider the resulting data as a function of both depression angle and azimuth (or "viewing") angle.

15. SUBJECT TERMS
Electromagnetic modeling, Human RCS

16. SECURITY CLASSIFICATION OF:			17. LIMITATION OF ABSTRACT	18. NUMBER OF PAGES	19a. NAME OF RESPONSIBLE PERSON
a. REPORT	b. ABSTRACT	c. THIS PAGE	UU	14	Kenneth Ranney
Unclassified	Unclassified	Unclassified			19b. TELEPHONE NUMBER (*Include area code*) 301-394-0832

Contents

List of Figures

1. Introduction

Researchers at the U.S. Army Research Laboratory (ARL) recently leveraged X-patch modeling tools to create moving target indicator (MTI) signatures of a walking man. In particular, we identified the modeling modifications required to generate representative signatures for an array-based system operating in the far field. We also generated radar signatures of a walking man at multiple depression angles, multiple viewing (i.e., azimuth) angles, and the multiple positions that constituted the man's walking motion. In what follows, we describe these experiments and present the resulting preliminary data analysis.

2. Modeling the Walking Man

The electromagnetic (EM) modeling data leveraged for this investigation was generated using X-patch EM-solvers (*1*). We based our decision to use X-patch on earlier comparisons of results generated by both X-patch and the more rigorous ARL finite difference time domain (AFDTD) method (*2*). These earlier results indicated that the differences between X-patch and the AFDTD were not significant enough to warrant trading computational speed for accuracy—an important consideration, since we required a large number of signatures.

We began by creating the necessary facet model (meshes) of the walking man at a specific viewing angle and a specific depression angle. We then repeated the procedure at 40 distinct positions within one-half of the walking cycle, as illustrated in figure 1 (*3*). Here we have defined a walking cycle to include two steps—one with the right foot and the second with the left. Finally, we altered the viewing (azimuth) angle and the depression angle, enabling us to systematically examine the target signature variability as a function of these parameters. Since we intended to mimic an array of transmit/receive elements operating at large standoff distances, we also required a very fine angular spacing. In fact, the angular offsets between array elements at realistic target ranges became so small that the changes from one element to the next became indiscernible. This effect is also evident in the imagery (considered in the next section) that provides some insight into the nature of the walking man's signature.

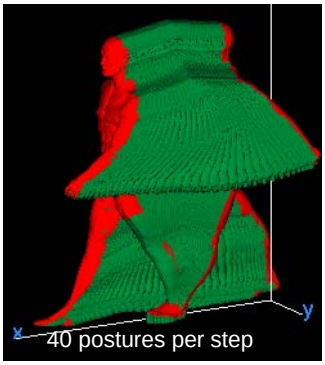

Figure 1. Samples from half of the walking cycle used to generate the moving target. The various postures are indicated in green.

For our initial experiments, we considered a limited set of depression angles in order to reduce the number of variables to a manageable level. We fixed our depression angles at 15° and 30°—values representative of those encountered by the Foliage Penetrating, Reconnaissance, Surveillance, Tracking, and Engagement Radar (FORESTER) system. In addition, we considered azimuth angles that were separated by approximately 0.04°, and examined signatures as a function of both azimuth (viewing angle) and frequency, where frequency varied over the range of 400–500 MHz. We always considered only horizontal (HH) polarization for these experiments because the FORESTER system is horizontally polarized. Figure 2 includes examples of target meshes for several azimuth angles.

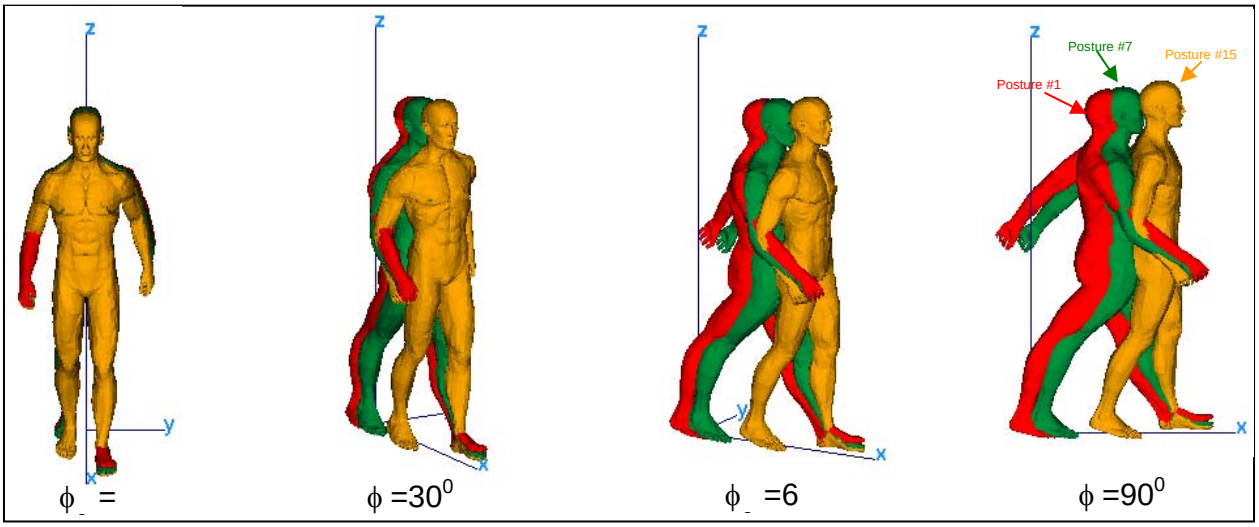

Figure 2. Examples of target postures viewed at different azimuth angles, where ϕ denotes azimuth. Each "posture" denotes a particular pose within the set of 40 poses constituting one-half of a walking cycle. Each walking cycle consists of two strides—one with the left foot and one with the right foot.

As part of our signature generation, we considered the man to be solid, with a uniform dielectric constant of

$$\varepsilon_r = 50 - j12 \quad (1)$$

We based this approximation on earlier work that demonstrated it to be reasonable (*2*). The man was also assumed to walk on a flat ground with dielectric constant equal to

$$\varepsilon_r = 8 \quad (2)$$

3. Data Evaluation

In order to evaluate effects of target orientation on the expected radar return, we examined the walking man's radar cross section (RCS) as a function of both azimuth angle and depression angle for a HH polarized radar. These results are displayed in figures 3 and 4 for the 15°- and 30°-depression angles, respectively, for a select subset of postures. In each figure, the top row of images displays RCS over a 180° range of azimuth angles, while the bottom row of images shows an expanded view around azimuth angles near 0°. It should be noted that the color scale for the bottom row of images in figure 3 differs radically from the color scale for the top row of images in figure 3, as indicated by the color bar at the right side of each row.

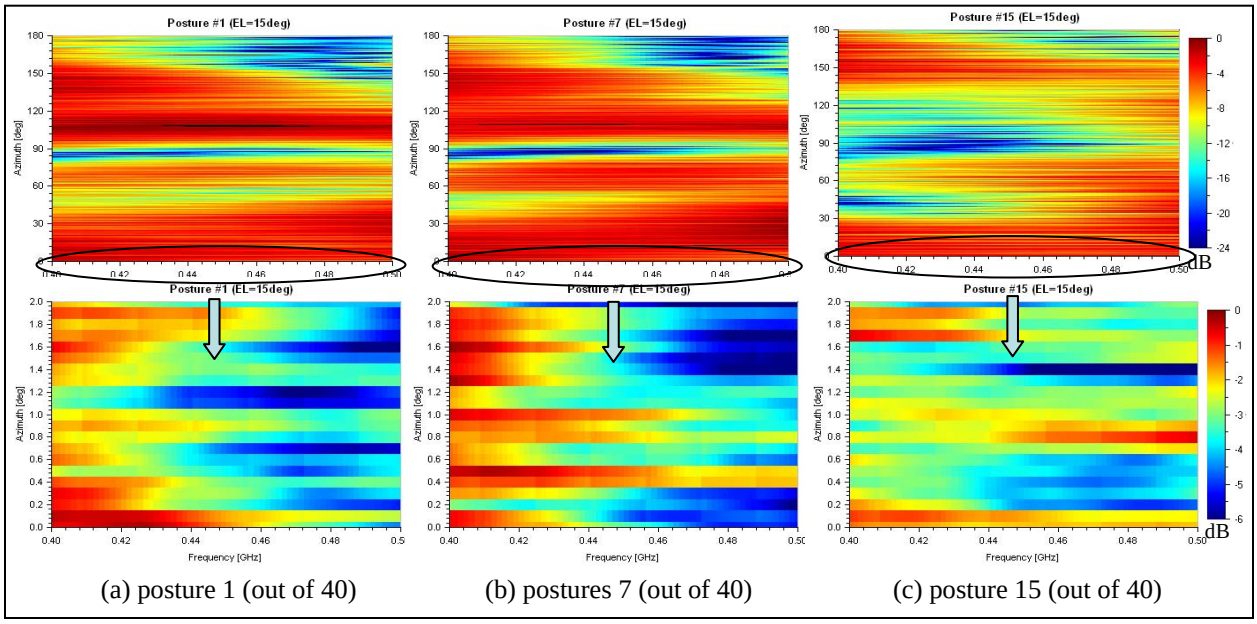

(a) posture 1 (out of 40) (b) postures 7 (out of 40) (c) posture 15 (out of 40)

Figure 3. RCS as a function of frequency (in GHz) and azimuth (in degrees) for a 15° depression angle, horizontally polarized radar. Images in the first row correspond to postures 1, 7, and 15 out of the 40 postures available within half of a walking cycle. Images in the second row show a zoomed view of the approximate area within the ellipses of the first row.

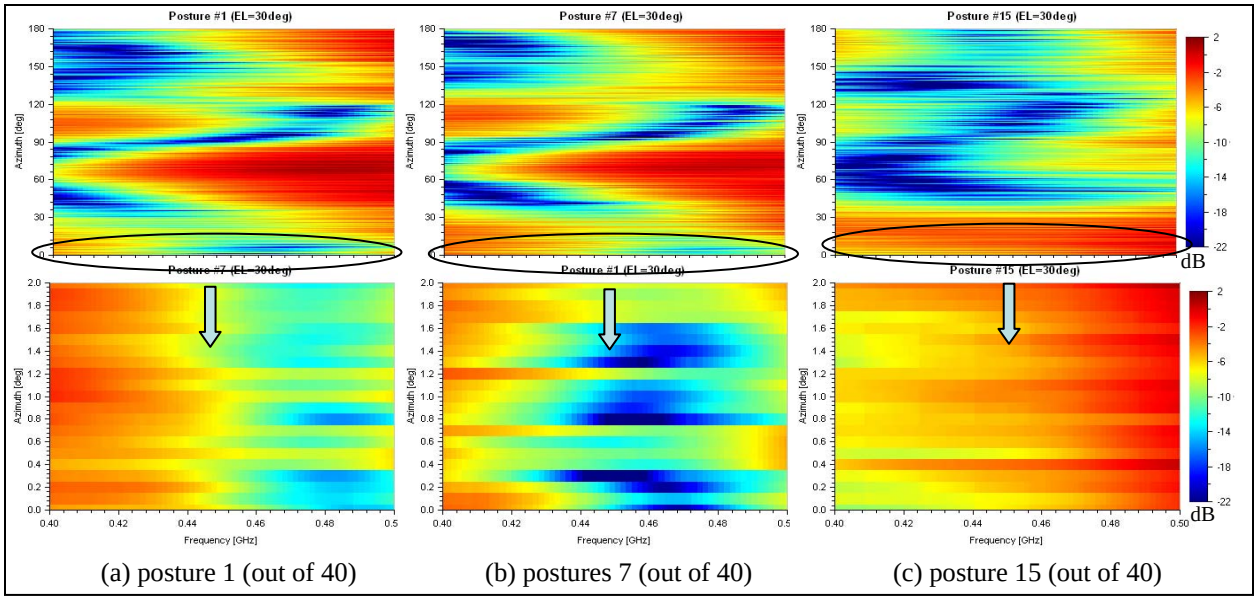

Figure 4. RCS as a function of frequency (in GHz) and azimuth (in degrees) for a 30° depression angle, horizontally polarized radar. Images in the first row correspond to postures 1, 7, and 15 out of the 40 postures available within half of a walking cycle. Images in the second row show a zoomed view of the approximate area within the ellipses of the first row.

From these images we inferred that the amount of energy reflected by the walking man is dependent upon both frequency and azimuth angle. In particular, the amount of variation at the higher depression angle could be particularly severe across a range of azimuth angles for all three of the examined poses. This effect became somewhat less severe at lower depression angles, as illustrated in the imagery of figure 3 for an azimuth angle of nearly 0°. Here we observed a dynamic range of only about 6 dB compared with a dynamic range of roughly 22 dB for similar azimuth angles in figure 4.

Initially, we expected there to be a high degree of symmetry between the RCS values observed at 0° and those observed at 180°; however, this was not the case for the postures considered in figures 3 and 4. In order to determine the effect of the arm and leg articulations on the generated RCS values for these postures, we considered an additional, static pose, denoted “posture 0” and shown in figure 5. Note that this pose could not be encountered in practice, since both feet are together and in contact with the ground. For this reason, posture 0 eliminated the effects due to arm and leg extension during walking, and provided us with a baseline for determining the amount of symmetry between signatures collected from the front and from the back.

Figure 5. Position of the man for "posture 0". Note that both feet are together and in contact with the ground, making this an impossible position to achieve as part of a normal walking motion.

As with the earlier postures, we generated RCS values as a function of both azimuth angle and frequency for posture 0. This time we considered two different depression angles—0° and 15°—in order to best observe the effects that were of interest, and the resulting imagery is displayed in figure 6. We observed the anticipated front-to-back symmetry across all frequencies when viewing the man at 0° depression, as evidenced by the imagery in figure 6(a). This symmetry remained, to some extent, when we increased the depression angle to 15°; even though, at 15° the man no longer exhibited the "box-like" configuration that yielded nearly constant RCS as a function of frequency. Still, the RCS values at the 15° depression angle remained similar across all frequencies. When contrasted to the more random-looking RCS data in figures 3 and 4, we see the effect of the out-of-plane scattering by the arms and legs (that is, out-of-plane relative to the head and torso). This indicates a substantial amount of scattering coming from the arms and legs, relative to the torso scattering.

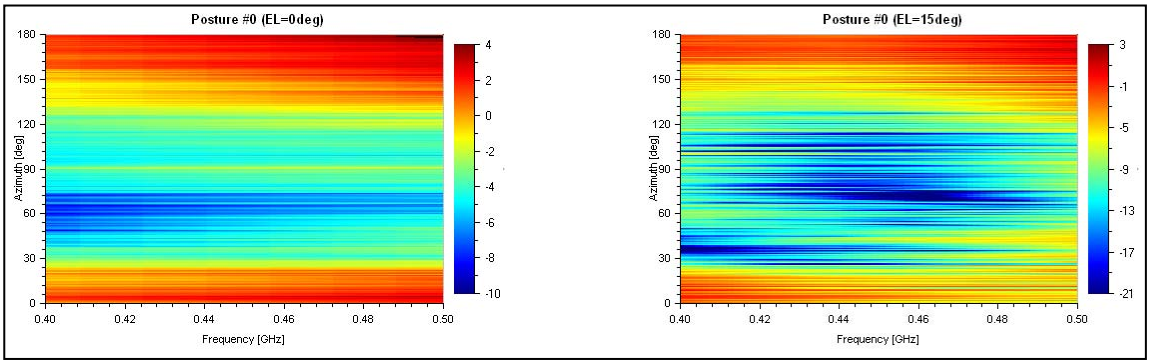

Figure 6. RCS values generated for the man at "posture 0". The expected front-to-back symmetry across all frequencies is particularly evident at 0° depression angle. While increasing the depression angle disrupts (somewhat) the uniformity of the response across frequency, we still note generally higher RCS values when the man is viewed from either the front or the back.

Finally, when we considered the walking man's RCS as a function of azimuth, we noted that small changes in azimuth (on the order of 0.1°) resulted in small changes in RCS. This would

imply relatively consistent signal levels across the range of azimuth values likely to be measured in practice. While this would be desirable for achieving high signal levels across a coherent processing interval (CPI), we also observed azimuth angles that produced lower RCS at the frequencies of interest. The fact that these azimuth angles occurred near 90° could prove to be problematic, since this direction of motion also produces the lowest Doppler-domain separation from the stationary clutter background. We also noted that the lack of angular diversity available across the array at long ranges implied that our standard methods for locating the target in cross-range—based on near-range measurements collected with ARL's synchronous impulse reconstruction (SIRE) radar (*4*)—would not provide adequate resolution. Extensive modifications would be required to address this issue.

4. Conclusion

We leveraged X-patch EM-solvers to generate an extensive set of moving target signatures and described certain characteristics of these signatures. In particular, we generated synthetic radar signatures from a walking man at finely spaced azimuth angles over a range of frequencies between 400 and 500 MHz. The man's motion was represented by a set of poses captured at 40 different instants within one half of the walking cycle, where we considered a walking cycle to consist of two strides—one with the left foot and one with the right. We generated data according to this model in order to approximate measurements collected by an array of transmit/receive elements operating at long stand-off ranges. We then used this synthetic data to examine characteristics of the walking-man signature at depression angles of 15° and 30°.

The synthetic data indicated that—as a function of azimuth—the amount of variation in the expected RCS of the walking man was more severe at the higher depression angle; however, the amount of variation within the range of azimuth angles encountered for a single target realization was negligible. When we zoomed in on a set of low azimuth angles at a depression angle of 15°, the relative RCS stability at 15° became even more apparent; all of the RCS values generated at 15° were within 6 dB of the peak value. In fact, the 15° depression angle seemed to be most favorable for target detection, with significant anticipated problems only if the target were to move along a line perpendicular to the radar's line of sight. Unfortunately, this target orientation also results in the lowest Doppler-frequency separation between target and clutter and, hence, a lower probability of detection. This suggested that the depression angles likely encountered by FORESTER are more favorable for target detection.

The modeled data created here proved useful for examining underlying characteristics of the walking-man signature. Future work could very well leverage this asset in the pursuit of ever-improving automatic target detection algorithms.

5. References

1. XPATCH User's Manual, SAIC/DEMACO, Champaign, IL. (This document is export controlled, available to U.S. Government users and DoD Contractors only).

2. Dogaru, T.; Le, C. *Validation of Xpatch Computer Models for Human Body*; ARL-TR-4403; U.S. Army Research Laboratory: Adelphi, MD, March 2008.

3. Dogaru, T.; Le, C.; and Kirose, G. *Time-frequency Analysis of a Moving Human Doppler Signature*; ARL-TR-4728; U.S. Army Research Laboratory: Adelphi, MD, February 2009.

4. Ranney, K.; Martone, A.; Nguyen, L.; Stanton, B.; Ressler, M.; Wong, D.; Koenig, F.; Tran, C.; Kirose, G.; Smith, G.; Kappra, K.; Sichina, J. Recent MTI Experiments Using ARL's Synchronous Impulse Reconstruction (SIRE) Radar. *Proc. of SPIE*, vol. 7308, 2009, pp. 73080Q-1–73080Q-12.

NO. OF COPIES	ORGANIZATION
1 ELEC	ADMNSTR DEFNS TECHL INFO CTR ATTN DTIC OCP 8725 JOHN J KINGMAN RD STE 0944 FT BELVOIR VA 22060-6218
1	DARPA ATTN IXO S WELBY 3701 N FAIRFAX DR ARLINGTON VA 22203-1714
1 CD	OFC OF THE SECY OF DEFNS ATTN ODDRE (R&AT) THE PENTAGON WASHINGTON DC 20301-3080
1	US ARMY INFO SYS ENGRG CMND ATTN AMSEL IE TD A RIVERA FT HUACHUCA AZ 85613-5300
1	COMMANDER US ARMY RDECOM ATTN AMSRD AMR W C MCCORKLE 5400 FOWLER RD REDSTONE ARSENAL AL 35898-5000
1	US ARMY RSRCH LAB ATTN RDRL CIM G T LANDFRIED BLDG 4600 ABERDEEN PROVING GROUND MD 21005-5066
16	US ARMY RSRCH LAB ATTN IMNE ALC HRR MAIL & RECORDS MGMT ATTN RDRL CIM L TECHL LIB ATTN RDRL CIM P TECHL PUB ATTN RDRL SER U C TRAN ATTN RDRL SER U D WONG ATTN RDRL SER U F KOENIG ATTN RDRL SER U G KIROSE ATTN RDRL SER U G SMITH ATTN RDRL SER U K KAPPRA ATTN RDRL SER U K RANNEY (4 COPIES) ATTN RDRL SER U L NGUYEN ATTN RDRL SER U M RESSLER ATTN RDRL SER U R INNOCENTI ADELPHI MD 20783-1197

TOTAL: 22 (1 ELEC, 1 CD, 20 HCS)